Running Title: *CCL22* upregulation in cancer cells via paracrine signaling

Title: Tumor cells upregulate *CCL22* in a STING-dependent manner in response to paracrine factors released by STING-activated myeloid cells and type I interferons

Elmira M Lomashvili[1], Jihyun Kim[2], Lingwei Kong[1], Pamela R. Cook[1]*

[1]Department of Biomedical Sciences, Mercer University School of Medicine, Macon, GA, USA

[2]Department of Biomedical Sciences, Mercer University School of Medicine, Columbus, GA, USA

*Corresponding: Pamela R. Cook cook_p@mercer.edu

ABSTRACT

Immunosuppressive elements within the tumor microenvironment include both regulatory T cells (Tregs) and M2 macrophages. A well-described mechanism of Treg recruitment occurs via the chemokine CCL22, and CCL22 has also recently been implicated in the polarization of tumor-associated macrophages to the M2a subtype. Our lab and others have shown that CCL22 is upregulated in cancer cells following activation of the STimulator of INterferon Genes (STING). STING triggers immune responses against pathogenic and self-DNA mislocalized to the cytoplasm, which can accumulate in cancer cells due to chromosomal instability, damaged mitochondria, and increased expression of LINE-1 retrotransposons. STING activation has been associated with both anti- and pro-tumor immune responses, and a potential mechanism of STING-mediated immune evasion is through CCL22 upregulation. CCL22 was first characterized in macrophages, and here we investigate the effects of STING activation on *CCL22* expression in macrophages and monocytes. We report that human macrophages and monocytes are resistant to *CCL22* upregulation by STING, but that STING-activated macrophages and monocytes release unidentified paracrine factor(s) that dramatically increase *CCL22* upregulation in cancer cells in a manner that remains STING-dependent, as evidenced by the inability of STING knockout cells to upregulate *CCL22* in response to these factors. We further found that exogenous type I interferons (IFNs), a major downstream product of STING activation, also upregulate *CCL22* in cancer cells via a STING-dependent mechanism and that exogenous IFNβ can directly activate STING.

32 **INTRODUCTION**

33 The STimulator of INterferon Genes (STING) is an effector protein that transmits signals
34 from various cytosolic DNA sensors to transcription factors, including interferon regulatory
35 factor 3 (IRF3), which leads to the expression of type I interferon (*IFN*) genes and downstream
36 immune responses (1-3). Healthy, non-mitotic eukaryotic cells confine DNA to the nucleus and
37 mitochondria; thus, the presence of cytosolic DNA often signals infection by microbes, making
38 STING an important sentinel in innate immune surveillance. Cancer cells are often characterized
39 by self-DNA mislocalized to the cytoplasm due to chromosomal instability, damaged
40 mitochondria, and reactivated LINE-1 retrotransposons (4, 5). LINE-1-mediated activation of
41 STING is thought to contribute to inflammation in multiple disease states, including age-related
42 neuropathologies and cancer (5-8). In the context of cancer, LINE-1 is highly expressed in many
43 epithelial tumors (9-11), and its activation of STING in those cells may have important clinical
44 implications on host anti-tumor immune responses. STING activation in cancer can boost anti-
45 tumor immunity due to the release of type I IFNs, and indeed STING agonists represent
46 promising immunotherapy agents (12, 13). However, the roles of STING in carcinogenesis,
47 tumor progression, and metastasis are complex, and in some cases STING activation has been
48 associated with impaired anti-tumor immunity (14-16).

49 Our lab and others have demonstrated a link between STING activation and increased
50 expression of a chemokine associated with immunosuppression in the tumor microenvironment,
51 the C-C-motif ligand 22 (*CCL22*) (17-19). Correlations between *CCL22* expression and adverse
52 outcomes across various cancer types have been reported in multiple studies (18, 20-24),
53 although CCL22 has also been associated with increased patient survival in some cancers,
54 particularly for colon and head and neck squamous cell carcinomas (19 and references therein).

55 CCL22 recruits regulatory T-cells (Tregs) via its interaction with the CCR4 receptor, which may
56 reduce tumor immune responses and promote immunosuppression in some cancers (25, 26).
57 Recently, CCL22 has also been reported to have a role in polarizing tumor-associated
58 macrophages to the M2a pro-tumor subtype (27).

59 CCL22, also known as macrophage-derived chemokine (MDC), was originally
60 discovered in macrophages (28, 29). Macrophages and other myeloid cells are major targets of
61 STING agonists in the tumor microenvironment (27). Here we sought to investigate the
62 relationship between STING activation and *CCL22* upregulation in macrophages and monocytes.
63 Although we found that STING activation did not increase *CCL22* expression in macrophages or
64 monocytes, we found that factor(s) released from these myeloid cells dramatically upregulated
65 *CCL22* in cancer cells in a paracrine fashion. Moreover, we determined that this paracrine effect
66 remains dependent on STING in the cancer cells, based on results from our STING knockout cell
67 line. We previously showed that *CCL22* upregulation in response to STING activation occurs
68 predominantly via the STING-IRF3 axis (19), the same axis that triggers robust upregulation of
69 type I IFNs. We thus hypothesized that type I IFNs could be the relevant paracrine factor(s)
70 released by myeloid cells that upregulate *CCL22* in cancer cells. Although we found that
71 exogenous type I IFNs did indeed increase *CCL22* expression in cancer cells, the myeloid-
72 derived paracrine factors tended to have a larger effect, particularly in HeLa cells. Surprisingly,
73 we also found that upregulation of *CCL22* in response to type I IFNs remained dependent on
74 STING, and that IFNβ itself could activate STING.

75 **MATERIALS AND METHODS**

76

77 **Cells and cell culture**

78 Cell lines used in the study include MCF7 (human mammary gland adenocarcinoma), THP-1
79 (human monocytic leukemia), both purchased from ATCC, human HeLa cervical
80 adenocarcinoma cells, a kind gift from Dr. Anthony Furano from the National Institute of
81 Diabetes and Digestive and Kidney Diseases as described in (19), and HeLa$^{-/-TMEM173}$ STING
82 *(TMEM173)* knockout cells, engineered from the aforementioned wild type HeLa with the
83 CRISPR-Cas 9 system, also described in (19). All cells were cultured in DMEM high glucose
84 with GlutaMAX and pyruvate (Gibco, cat. 10569010) supplemented with 10% fetal bovine
85 serum (Gibco OneShot, non-heat-inactivated, cat. A3160401) and 1x antibiotic-antimycotic (100
86 units/mL penicillin, 100 ug/mL streptomycin, 0.25 ug/mL Amphotericin B; Gibco, cat.
87 15240096) in a humidified incubator at 37°C with 5% CO_2. THP-1 culture media was
88 additionally supplemented with 1x 2-mercaptoethanol (Gibco, cat. 21985023).

89

90 **Cell culture treatments (STING agonists, IFNα, IFNβ, and MMHAR-2 block)**

91 Four commercially available STING agonists were used in the study: a stabilized analog of the
92 cyclic dinucleotide canonical STING agonist 2'3'-cGAMP (2'3'-cGAM(PS)2(Rp/Sp)), hereafter
93 referred to as cGAM(PS)2 (Invivogen, cat. tlrl-nacga2srs), a stabilized cyclic adenine
94 monophosphate-inosine monophosphate (cAIM(PS)2 Difluor (Rp/Sp), hereinafter referred to as
95 cAIM(PS)2 (Invivogen, cat. tlrl-nacairs-2), E7766, a macrocycle-bridged diammonium salt
96 (Chemietek, cat. CT-E7766), and the diamidobenzimidazole diABZI (Selleckchem, cat.
97 S8796). All agonists except diABZI were water soluble and reconstituted using a companion

98 vial of sterile, endotoxin-free LAL water; diABZI was reconstituted in dimethyl sulfoxide
99 (DMSO). All agonists were diluted to a final concentration of 30 uM in complete cell culture
100 media and applied to cells as specified in the figures. Human recombinant IFNα stock (pbl assay
101 science, cat. 11101-1) was diluted to concentrations indicated in the figure legends in complete
102 cell culture media. Lyophilized recombinant human IFNb (PeproTech, cat. 300-02) was initially
103 reconstituted in sterile, endotoxin-free LAL water and further diluted into sterile 0.1% bovine
104 serum albumin (BSA) in 1x phosphate-buffered saline (PBS) to 100 ng/uL and further diluted to
105 concentrations indicated in the figure legends in complete cell culture media before adding to
106 cells. MMHAR-2 blockade was performed by pretreating cells with 8.3 µg/mL of the MMHAR-
107 2 antibody, then adding indicated treatments diluted in cell culture media, reducing the final
108 concentration of MMHAR-2 to 5 µg/mL. Cells were then incubated for approximately 30 hours
109 prior to harvesting for either Western blots or RTqPCR.
110
111 **Macrophage differentiation and generation of conditioned media**
112 THP-1 cells were differentiated into macrophages by plating cells in complete culture media
113 supplemented with 150 nM phorbol 12-myristate 13-acetate (PMA) and incubating for 96 hours,
114 with one media change performed after 48 hours to replenish PMA. PMA-containing media was
115 then removed, and cells were allowed to rest for 24 hours prior to treatment with cGAM(PS)2.
116 Conditioned media from both macrophages and undifferentiated monocytes was obtained by
117 treating cells with fresh complete media, with or without the addition of 30 uM cGAM(PS)2,
118 incubating for 24 hours, then gently removing media, centrifuging at 300 x g, and transferring to
119 cancer cells.
120

121 **Cell imaging**

122 The morphological changes during THP-1 differentiation were imaged using an EVOS FLoid
123 system.

124

125 **RNA purification and RTqPCR**

126 Cells were harvested using TRIzol reagent (Invitrogen, cat. 15596026) followed by column RNA
127 purification and on-column DNase digestion according to the TRIzol two-step protocol from the
128 Monarch total RNA miniprep kit (NEB, cat. T2010S). Purity and concentration of the RNA were
129 assessed using spectrophotometry. First-strand cDNA synthesis was performed using the
130 LunaScript RT SuperMix Kit (NEB, cat. E3010S) or LunaScript (-) RT SuperMix control with
131 added M-MuLV Reverse Transcriptase (NEB). qPCR was performed on a QuantStudio 3 real-
132 time PCR machine using TaqMan Fast Advanced Master Mix (Applied Biosystems, cat.
133 A44359). Singleplexed and duplexed 5' endonuclease assays were performed using the
134 following TaqMan Assays: *CCL22* (Hs00171080); IFN-β (Hs01077958_s1; beta actin
135 (Hs99999903); and 18s (Hs99999901). For duplexed assays, a beta-actin primer-limited assay
136 (IDT) was used. Samples for qPCR were assayed in technical triplicates, and data were analyzed
137 with the delta-delta Ct method; when multiple housekeeping genes were measured, their
138 combined geometric mean was used for analysis.

139

140 **Cell lysis and Western blotting**

141 Cells were lysed for immunoblotting in 3% SDS, 25 mM Tris-HCl pH 7.4, and 0.5 mM EDTA
142 supplemented with 3X HALT protease and phosphatase inhibitor cocktail (ThermoFisher, cat.
143 78440). Lysate homogenization was achieved with QIAshredder columns (Qiagen, cat. 79656),

144 after which protein concentration was determined using the BioRad DC Protein Assay (cat.
145 5000112). Equal amounts of lysates were resolved with SDS-PAGE. Transfers were performed
146 using a wet tank system overnight at 28 V or the BioRad Trans-Blot Turbo Transfer system.
147 Blots were imaged with an infrared Li-Cor Odyssey CLx Imager and processed using Image
148 Studio (Li-Cor). Positive controls for phospho-STING (S366) were prepared as commercially
149 described by transfecting THP-1 differentiated macrophages with dsDNA (pcDNA3.1 (+) puro),
150 (3.33 ug/mL) using Opti-MEM (Gibco, cat. 31-985-062) as the DNA diluent and TransIT-LT1
151 (Mirus, cat. MIR 2300) at a ratio of 1 ug DNA: 2 uL TransIT-LT1; cells were harvested 4 hours
152 after transfection with the lysis buffer described above.
153
154 **Antibodies**
155 Antibodies for Western blots included: anti-phospho(S366)-STING (Cell Signaling Technology,
156 cat. 19781S); anti-phospho(Y701)-Stat1 (Cell Signaling Technology, cat. 9167); anti-IFNAR2
157 (Cell Signaling Technology, cat. 53883); and anti-beta-tubulin (Abcam, cat. ab6046). The
158 antibody used for IFNAR blockade was anti-human interferon alpha/beta receptor chain 2, clone
159 MMHAR-2 (pbl assay science, cat. 21385-1).
160
161 **Statistical analyses**
162 Statistical analyses were performed using GraphPad Prism 9. Tests for significance are described
163 in the figure legends, and statistical significance was defined as p-value ≤ 0.05.
164

165 **RESULTS**

166

167 **STING-activated macrophages and monocytes do not upregulate *CCL22*.** Macrophages are a
168 major source of CCL22, reflected in the historical name of CCL22, macrophage-derived
169 chemokine (MDC). Since one of the targets of STING agonists are tumor-associated
170 macrophages, we sought to determine the effect of STING activation on *CCL22* in these cells.
171 Using the well-established THP-1 monocyte-to-macrophage differentiation model (Fig. 1A), we
172 incubated THP-1 monocytes with phorbol myristate acetate (PMA) for four days to establish
173 adherent, differentiated macrophages. Following differentiation, we treated the THP-1-derived
174 macrophages with the canonical human STING agonist cGAM(PS)2 for 24 hours.
175 Unexpectedly, we found that cGAM(PS)2 did not increase *CCL22* expression but rather reduced
176 it (Fig. 1B). To ensure that we had not missed an increase in *CCL22* at an earlier time point, we
177 monitored *CCL22* expression at 0, 6, 12, 24, and 48 hours, which revealed no significant increase
178 at any time point (Fig. S1). Rather, the time course in Fig. S1 shows a downward trend in *CCL22*
179 expression, although these decreases did not reach statistical significance in the context of a
180 Kruskal-Wallis multiple comparisons test, which generally has less power to identify differences
181 in means compared with the *t* test used to analyze data in Figure 1B. Indeed, when analyzing
182 only the 24-hour time-course data with an unpaired, two-tailed *t* test, the decrease in *CCL22* was
183 again significant ($p = 0.0290$). To determine whether failure to activate *CCL22* in macrophages
184 was due to a lack of STING activation, we confirmed that cGAM(PS)2 induced STING
185 phosphorylation in macrophages at both 6 and 24 hour time points (Fig. 1C). Consistent with
186 results from macrophages, undifferentiated THP-1 monocytes also failed to upregulate *CCL22* in
187 response to cGAM(PS)2 (Fig. 1D).

188

189 **STING-activated macrophages and monocytes release factor(s) that upregulate *CCL22* in**
190 **cancer cells.** Macrophages have important roles in anti-tumor immunity but can also contribute
191 to immunosuppressive environments (30). We thus sought to determine whether STING-
192 activated macrophages might release factors that could act via paracrine signaling to alter *CCL22*
193 expression in cancer cells. *CCL22* has been reported to play a role in breast (20, 22, 24) and
194 cervical (18, 23) cancers, and we used human breast (MCF7) and cervical (HeLa) cancer cells in
195 these experiments. These cell lines were also used in our previous study, where we showed that
196 both CCL22 mRNA and protein were increased upon direct STING activation with cytosolic
197 DNA or cGAM(PS)2 (19). To investigate potential paracrine activation of *CCL22* in these cells,
198 we first treated macrophages with cGAM(PS)2 or a mock control for 24 hours, then removed the
199 media and applied it to cancer cells for 24 hours. Both MCF7 (Fig. 2A) and HeLa cells (Fig. 2B)
200 exposed to conditioned media from macrophages treated with cGAM(PS)2 exhibited a robust
201 increase in *CCL22* compared to media from untreated macrophages or treatment with
202 cGAM(PS)2 alone, although conditioned media from untreated macrophages also increased
203 *CCL22* in HeLa cells, albeit to a lower extent. Monocytes also released factors that increased
204 *CCL22* above levels induced by direct STING activation in MCF7 (Fig. 2C) and HeLa (Fig. 2D)
205 cells.

206

207 **Paracrine activation of *CCL22* in cancer cells activates STING and is dependent on STING.**
208 Our previous study showed that *CCL22* upregulation in response to cytosolic dsDNA and
209 cGAM(PS)2 in HeLa cells was dependent on STING. However, in the current experiments, it
210 was possible that paracrine-mediated activation of *CCL22* in these cells was independent of

211 STING. To investigate this, we first determined whether conditioned media from STING-
212 activated macrophages had any effect on STING activation in HeLa cells, as determined by
213 analysis of STING phosphorylation on serine 366 (31, 32). Figure 3A shows that STING in
214 HeLa cells was indeed activated by media obtained from STING-activated macrophages, and
215 this activation was greater than when HeLa cells were treated directly with cGAM(PS)2.
216 Importantly, in our previous study, we confirmed that free-floating DNA, which could possibly
217 have been present in the conditioned media, did not activate STING in HeLa cells (19). Notably,
218 the degree of STING activation by each treatment in Figure 3A generally corresponds to relative
219 levels of *CCL22* upregulation in Figure 2B, including the slight increases observed in response to
220 media from untreated macrophages. Similar results for STING phosphorylation were observed
221 when treating HeLa cells with conditioned media from monocytes (Fig. S2A), which again
222 parallels increases in *CCL22* in Figure 2D. Note that we did not examine STING
223 phosphorylation on S366 in MCF7 cells due to our previous finding that STING activation in
224 MCF7 cells with cytosolic dsDNA or pharmacological agonists occurred in the absence of
225 phosphorylation on S366 for unknown reasons, which are further discussed in that study (19). To
226 determine whether the observed STING activation was *required* for paracrine-mediated
227 upregulation of *CCL22*, we used a STING (gene name *TMEM173*) knockout cell line, HeLa$^{-/-}$
228 ^{TMEM173}, which we previously established and characterized from the parental HeLa cells used
229 here (19). Treatment of the HeLa$^{-/-TMEM173}$ STING knockout cells with media from STING-
230 activated macrophages showed no statistically significant increase in *CCL22* expression,
231 indicating that intact STING signaling in the cancer cells was still required for upregulated
232 *CCL22* (Fig. 3B). Similar results were obtained using media from STING-activated monocytes
233 (Fig. S2B).

234

235 **Type I IFNs have modest effects on *CCL22* in HeLa cells that remain STING-dependent.**

236 We previously found that STING-mediated *CCL22* upregulation in HeLa cells is mediated
237 predominantly via the STING-IRF3 axis, which triggers robust expression of type I IFNs (19).
238 We therefore hypothesized that the relevant paracrine factor(s) leading to the increase in *CCL22*
239 might be type I IFNs. Overall however, IFNα failed to elicit strong *CCL22* expression in either
240 cell type, and effects of IFNβ plateaued in dose-response curves, indicating that the relevant
241 paracrine factor was unlikely a higher concentration of type I IFNs.

242 In HeLa cells, IFNβ did not significantly upregulate *CCL22* at any dose at 24 hours (Fig.
243 S3A), and subsequent time-course analyses indicated the maximum response to both IFNα and
244 IFNβ occurred at 48 hours. However, even at 48 hours, IFNα failed to significantly upregulate
245 *CCL22* in HeLa cells except at the highest dose (100 ng/mL), and then only to an average of 15
246 fold (Fig. 4A). IFNβ increased *CCL22* at the lowest dose (1 ng/mL) in HeLa cells, but only to
247 approximately 10 fold, and higher doses of IFNβ failed to elicit any additional increase (Fig. 4B).
248 MCF7 cells upregulated CCL22 in response to type I IFNs more rapidly than HeLa cells,
249 showing higher levels at 24 hours compared to 48 hours (Fig. S3B). At the highest dose, IFNα
250 increased *CCL22* by an average of only 6.7 fold in 24 hours (Fig. 4C). Paralleling the relative
251 effects of IFNα and IFNβ in HeLa cells, IFNβ also increased *CCL22* in MCF7 cells more than
252 IFNα, with an average of 57 fold change in 24 hours at the highest dose (Fig. 4D). However, the
253 effect of IFNβ was still below that observed from paracrine activation of MCF7 cells by
254 conditioned media from STING-activated monocytes (76.5 fold, Fig. 2C), though it was slightly
255 above levels induced by conditioned media from STING-activated macrophages (46.3 fold, Fig.
256 2A).

257 We next tested the effect of exogenous IFNα and IFNβ on *CCL22* upregulation in the
258 context of STING knockout cells, HeLa$^{-/-TMEM173}$. Neither IFNα (Fig. 4E) nor IFNβ (Fig. 4F)
259 significantly affected *CCL22* expression in STING knockout cells. These data were unexpected
260 and indicate that the effect of exogenous IFNα and IFNβ on *CCL22* is dependent on STING.
261 Although STING is well-known to trigger expression of type I *IFNs* downstream of IRF3, to our
262 knowledge, a requirement of STING for the effects of exogenous type I IFNs has not been
263 reported. To determine whether STING was activated by type I IFN signaling, we treated wild-
264 type HeLa cells with IFNβ and then performed a Western blot to assess STING phosphorylation,
265 and indeed found that exogenous IFNβ resulted in activated STING (Fig. 4G). We did not test
266 the effect of IFNα due to the comparatively minimal effect we observed from IFNα on *CCL22*
267 relative to IFNβ. To rule out the possibility that type I IFNs failed to upregulate *CCL22* in the
268 STING KO cells due to an inadvertent disruption of the interferon receptor (IFNAR) and
269 downstream Stat1 signaling, we confirmed that our STING KO cells exhibited the same degree
270 of Stat1 phosphorylation in response to IFNα and IFNβ as wild-type cells (Fig. 4H). As
271 expected, we found that cGAM(PS)2, which activates STING and STING-mediated type I IFNs,
272 also slightly induced Stat1 in the wild-type cells, but this activation was blocked in the STING
273 KO cells, reflecting the lack of STING-mediated upregulation of type I IFNs available to bind
274 and activate the IFNAR-Stat1 pathway in those cells (Fig. 4H). Confirming intact pStat1
275 signaling in the STING KO cells is consistent with our hypothesis that *CCL22* upregulation in
276 response to exogenous type I IFN is mediated through STING, not Stat1. Given that Stat1
277 phosphorylation was equivalently induced in wild-type and STING knockout cells by type I
278 IFNs, it was also unlikely that IFNAR expression would have been reduced in the STING

279 knockout cells, but to confirm this, we also show equivalent levels of IFNAR in both cell lines
280 (S3C).
281 The inability of type I IFNs to activate *CCL22* expression in our STING KO cells,
282 combined with confirmation of intact IFNAR expression and signaling in STING KO cells,
283 indicated that *CCL22* upregulation in wild-type cells by type I IFNs occurs via STING. To
284 further examine the role of IFNAR signaling on *CCL22* activation in the context of type I IFNs,
285 direct STING activation with cGAM(PS)2, or paracrine activation using conditioned media, we
286 performed an IFNAR blockade using a well-characterized neutralizing monoclonal antibody
287 from PBL Assay Science, anti-human IFN-alpha/beta receptor chain 2, clone MMHAR-2. To
288 first confirm that MMHAR-2 exerted a neutralizing effect on IFNAR signaling, we analyzed the
289 ability of this antibody to reduce Stat1 phosphorylation in response to IFNα and IFNβ, as well as
290 cGAM(PS)2. MMHAR-2 somewhat reduced levels of phosphorylated Stat1 in response to
291 IFNα, but not IFNβ (Fig. S3D). This difference might be attributable to the reported higher
292 affinity of IFNβ for IFNARs compared to IFNα (33, 34). Given that cGAM(PS)2 upregulates
293 type I IFNs through its activation of STING, we also observed as expected that the MMHAR-2
294 blockade reduced Stat1 phosphorylation following treatment with cGAM(PS)2 (Fig. S3D). We
295 also confirmed that MMHAR-2 exerted no activating effect on Stat1 (Fig. S3E). After
296 establishing the neutralizing potential of MMHAR-2 in our system, we sought to determine the
297 contribution of IFNAR signaling to *CCL22* upregulation in response to type I IFNs,
298 cGAM(PS)2, and paracrine factors from STING-activated macrophages. Figure 4I shows the
299 relative degree of inhibition induced by MMHAR-2 for each treatment. Although not statistically
300 significant, MMHAR-2 produced an observable downward trend in *CCL22* expression for all
301 treatments except cGAM(PS)2. The neutralizing effect of MMHAR-2 was most noticeable in

302 cells treated with IFNα, where the p-value is approaching significance at 0.0659, and these
303 results parallel those observed for MMHAR-2 inhibition of IFNα-mediated Stat1
304 phosphorylation in Figure S3D. Also in Figure S3D, the very slight increase in Stat1
305 phosphorylation from cGAM(PS)2 treatment, as well as its return to baseline with MMHAR-2
306 pretreatment, most likely reflects the activity of cGAM(PS)2-induced type I IFNs downstream of
307 STING. That the IFNAR block had the least effect on *CCL22* upregulation by cGAM(PS)2 is
308 consistent with our other data indicating that *CCL22* upregulation downstream of STING in
309 HeLa cells is not mediated primarily or solely by type I IFNs.
310
311 **STING agonists differentially upregulate *CCL22* and *IFNβ***
312 We were curious, given the differential effects of type I IFNs and cGAM(PS)2 on *CCL22,*
313 whether different STING agonists would have distinctive effects on *CCL22* compared to *IFNβ*.
314 We tested a panel of four STING agonists that included two cyclic and two and non-cyclic
315 dinucleotides. The cyclic dinucleotides included cGAM(PS)2 and the stabilized analog of
316 adenosine-inosine monophosphate (cAIMP(PS)2) (35, 36). The two non-cyclic dinucleotides
317 were diamidobenzimidazole (diABZI) (37-39) and E7766, a locked, macrocycle-bridged agonist
318 (38, 40, 41). In HeLa cells, all agonists increased *CCL22* but had no significant effect on *IFNβ*
319 expression (Fig. 5A-5D). Three of the STING agonists increased *IFNβ* in MCF7 cells to
320 statistically significant levels, but *CCL22* was increased in response to all agonists, including
321 diABZI, the agonist that did not statistically increase *IFNβ* (Fig. 5E-5H). These results are
322 consistent with a mechanism of *CCL22* induction via STING that does not rely exclusively on
323 type I IFNs.
324

325 **DISCUSSION**

326 STING activation in tumors can promote anti-tumor immune responses, and STING
327 agonists represent an emerging class of immunotherapy agents (13, 42, 43). However, multiple
328 reports also indicate that STING can induce immunosuppressive tumor environments (reviewed
329 in 44). Several pro-tumor mechanisms of STING have been described, including upregulation of
330 programmed death ligand (44) and indoleamine 2,3-dioxygenase (45), radiation-induced
331 recruitment of myeloid suppressor cells (46), and DMBA exposure (47). One example of
332 immune equilibrium mediated by STING is the polarization of macrophages, where STING has
333 been reported to induce both anti-tumor M1 as well as pro-tumor M2 subtypes (44, 48, 49).

334 Our lab and others have found that STING activation can also increase expression of the
335 chemokine CCL22 in cancer cells (17-19). CCL22 is implicated in tumor immune evasion
336 through its recruitment of regulatory T cells (25, 26) and, more recently, by promoting
337 polarization of the M2 phenotype in tumor-associated macrophages (27). We previously showed
338 that STING activation by cytosolic dsDNA and the STING agonist cGAM(PS)2 can upregulate
339 *CCL22* expression in epithelial cancer cells via the STING-IRF3 axis (19). In the present study,
340 we show that macrophages and monocytes do not themselves upregulate *CCL22* in response to
341 STING activation but rather release unidentified factor(s) that in turn increase *CCL22* expression
342 in a paracrine fashion in cancer cells. STING-activated myeloid cells that can induce neighboring
343 cancer cells to upregulate CCL22 via paracrine signaling may thus contribute to
344 immunosuppressive tumor environments by favoring the recruitment of Tregs and polarization of
345 M2a macrophages.

346 Based on our prior finding that *CCL22* upregulation was downstream of the STING-IRF3
347 axis, we hypothesized that type I IFNs could be the relevant paracrine factor(s). However,

348 treatment of cancer cells with exogenous IFNα or IFNβ did not, in most cases, achieve the same
349 level of *CCL22* upregulation as conditioned media from STING-activated myeloid cells. For
350 example, in HeLa cells, treatment with type I IFNs increased *CCL22* by 10-20 fold, while
351 treatment with conditioned media from STING-activated macrophages increased *CCL22* by up
352 to 8,000 fold. In MCF7 cells, conditioned media from monocytes, but not macrophages, also
353 increased *CCL22* above levels induced by type I IFNs, although the effect was more modest.
354 Surprisingly, we found that *CCL22* upregulation by exogenous type I IFNs, as well as
355 paracrine factors, remained dependent on STING, as evidenced by the lack of *CCL22*
356 upregulation in STING knockout cells. Although STING-dependent expression of type I IFNs is
357 well-described, a requirement for STING for a functional effect of exogenous type I IFNs has, to
358 our knowledge, not been previously described. One possible explanation could be our finding
359 that IFNβ itself induces activating phosphorylation of STING, which also has not been
360 previously reported. However, other studies have indicated connections between type I IFNs and
361 the transcriptional regulation of *cGAS* and the gene that encodes STING, *TMEM173* (50, 51).
362 These findings raise important questions about feedback mechanisms between type I IFNs and
363 STING. Regarding such feedback, LINE-1 retrotransposons, which are reported to activate
364 cGAS-STING (5), were recently shown to be upregulated in both monocytes and neutrophils
365 exposed to IFNα (52). Many solid tumors upregulate LINE-1 expression (9, 53), making LINE-1
366 a possible source of CCL22 in cancer cells via cGAS-STING activation. The potential for
367 additional LINE-1 upregulation in myeloid cells by type I IFNs may further amplify STING
368 signaling in those cells, increasing the release of paracrine factors affecting *CCL22*.
369 More studies are needed to identify the paracrine factor(s) released from STING-
370 activated myeloid cells that induce *CCL22*. Multiple reports show that a variety of factors can

371 influence CCL22 regulation, including but not limited to IL-1, IL-4, IL-5, IFN-gamma (IFN-γ),
372 and tumor necrosis factor alpha (TNF-α), with some factors having different effects on CCL22
373 based on cell type (e.g. 28, 29, 54-59). A study in 2011 by Faget et al. showed that peripheral
374 blood mononuclear cells promoted increased secretion of CCL22 from breast cancer cells and
375 identified roles for monocyte-derived TNF-α and IL-1β, as well as exogenous IFN-γ (60).
376 Whether any of these factors, or combinations thereof, are among the paracrine factors released
377 by STING-activated myeloid cells in our study remains to be determined. However, one
378 important potential candidate, especially given the STING-dependency we observed for *CCL22*
379 upregulation in cancer cells, could be cGAMP itself. Intercellular transfer of cGAMP has been
380 shown to occur via several mechanisms, including cell-cell contacts such as phagocytosis and
381 gap junctions, as well as the release and uptake of cGAMP from the extracellular space through
382 various transport channels in the cell membrane (4, 61-65). Although these studies have largely
383 focused on cGAMP released by tumor cells that is taken up by myeloid cells, the converse may
384 also be true.

385 The findings presented here offer new insights into possible mechanisms of STING-
386 mediated immunosuppression in cancer. Future studies will be needed to determine clinical
387 associations between STING activation and increased intratumoral CCL22, and whether
388 increased levels of CCL22 in this context correlate with immunosuppression. In addition,
389 identification of the paracrine factor(s) released from STING-activated myeloid cells that can
390 increase CCL22 in cancer cells could reveal therapeutic strategies targeting Treg recruitment and
391 M2 polarization in solid tumors.

392 **REFERENCES**

393 1. Zhang, B., P. Xu, and A. Ablasser. 2025. Regulation of the cGAS-STING Pathway. *Annu*
394 *Rev Immunol* 43: 667-692.

395 2. Motwani, M., S. Pesiridis, and K. A. Fitzgerald. 2019. DNA sensing by the cGAS-
396 STING pathway in health and disease. *Nat Rev Genet* 20: 657-674.

397 3. Hopfner, K. P., and V. Hornung. 2020. Molecular mechanisms and cellular functions of
398 cGAS-STING signalling. *Nat Rev Mol Cell Biol* 21: 501-521.

399 4. Dvorkin, S., S. Cambier, H. E. Volkman, and D. B. Stetson. 2024. New frontiers in the
400 cGAS-STING intracellular DNA-sensing pathway. *Immunity* 57: 718-730.

401 5. Mathavarajah, S., and G. Dellaire. 2024. LINE-1: an emerging initiator of cGAS-STING
402 signalling and inflammation that is dysregulated in disease. *Biochem Cell Biol* 102: 38-
403 46.

404 6. Gamdzyk, M., D. M. Doycheva, C. Araujo, U. Ocak, Y. Luo, J. Tang, and J. H. Zhang.
405 2020. cGAS/STING Pathway Activation Contributes to Delayed Neurodegeneration in
406 Neonatal Hypoxia-Ischemia Rat Model: Possible Involvement of LINE-1. *Mol Neurobiol*
407 57: 2600-2619.

408 7. Gorbunova, V., A. Seluanov, P. Mita, W. McKerrow, D. Fenyo, J. D. Boeke, S. B.
409 Linker, F. H. Gage, J. A. Kreiling, A. P. Petrashen, T. A. Woodham, J. R. Taylor, S. L.
410 Helfand, and J. M. Sedivy. 2021. The role of retrotransposable elements in ageing and
411 age-associated diseases. *Nature* 596: 43-53.

412 8. De Cecco, M., T. Ito, A. P. Petrashen, A. E. Elias, N. J. Skvir, S. W. Criscione, A.
413 Caligiana, G. Brocculi, E. M. Adney, J. D. Boeke, O. Le, C. Beauséjour, J. Ambati, K.
414 Ambati, M. Simon, A. Seluanov, V. Gorbunova, P. E. Slagboom, S. L. Helfand, N.
415 Neretti, and J. M. Sedivy. 2019. L1 drives IFN in senescent cells and promotes age-
416 associated inflammation. *Nature* 566: 73-78.

417 9. Rodic, N., R. Sharma, R. Sharma, J. Zampella, L. Dai, M. S. Taylor, R. H. Hruban, C. A.
418 Iacobuzio-Donahue, A. Maitra, M. S. Torbenson, M. Goggins, M. Shih Ie, A. S. Duffield,
419 E. A. Montgomery, E. Gabrielson, G. J. Netto, T. L. Lotan, A. M. De Marzo, W. Westra,
420 Z. A. Binder, B. A. Orr, G. L. Gallia, C. G. Eberhart, J. D. Boeke, C. R. Harris, and K. H.
421 Burns. 2014. Long interspersed element-1 protein expression is a hallmark of many
422 human cancers. *Am J Pathol* 184: 1280-1286.

423 10. Burns, K. H. 2017. Transposable elements in cancer. *Nat Rev Cancer* 17: 415-424.

424 11. McKerrow, W., N. Doudican, N. Frazzette, S. A. Evans, A. Rocha, L. Kagermazova, J.
425 M. Sedivy, N. Neretti, J. Carucci, J. D. Boeke, and D. Fenyö. 2022. LINE-1
426 Retrotransposon expression in cancerous, epithelial and neuronal cells revealed by 5'
427 single-cell RNA-Seq. *bioRxiv*: 2021.2001.2019.427347.

428 12. Gan, Y., X. Li, S. Han, Q. Liang, X. Ma, P. Rong, W. Wang, and W. Li. 2021. The
429 cGAS/STING Pathway: A Novel Target for Cancer Therapy. *Front Immunol* 12: 795401.

430 13. Xu, Y., and Y. Xiong. 2024. Targeting STING signaling for the optimal cancer
431 immunotherapy. *Front Immunol* 15: 1482738.

14. Zhou, Z., S. Huang, F. Fan, Y. Xu, C. Moore, S. Li, and C. Han. 2024. The multiple faces of cGAS-STING in antitumor immunity: prospects and challenges. *Med Rev (2021)* 4: 173-191.

15. Samson, N., and A. Ablasser. 2022. The cGAS-STING pathway and cancer. *Nat Cancer* 3: 1452-1463.

16. Yue, B., W. Gao, J. F. Lovell, H. Jin, and J. Huang. 2025. The cGAS-STING pathway in cancer immunity: dual roles, therapeutic strategies, and clinical challenges. *Essays Biochem* 69.

17. Liang, D., H. Xiao-Feng, D. Guan-Jun, H. Er-Ling, C. Sheng, W. Ting-Ting, H. Qin-Gang, N. Yan-Hong, and H. Ya-Yi. 2015. Activated STING enhances Tregs infiltration in the HPV-related carcinogenesis of tongue squamous cells via the c-jun/CCL22 signal. *Biochim Biophys Acta* 1852: 2494-2503.

18. Ni, H., H. Zhang, L. Li, H. Huang, H. Guo, L. Zhang, C. Li, J. X. Xu, C. P. Nie, K. Li, X. Zhang, X. Xia, and J. Li. 2022. T cell-intrinsic STING signaling promotes regulatory T cell induction and immunosuppression by upregulating FOXP3 transcription in cervical cancer. *J Immunother Cancer* 10.

19. Kim, J., J. V. Pena, H. P. McQueen, L. Kong, D. Michael, E. M. Lomashvili, and P. R. Cook. 2024. Downstream STING pathways IRF3 and NF-kappaB differentially regulate CCL22 in response to cytosolic dsDNA. *Cancer Gene Ther* 31: 28-42.

20. Gobert, M., I. Treilleux, N. Bendriss-Vermare, T. Bachelot, S. Goddard-Leon, V. Arfi, C. Biota, A. C. Doffin, I. Durand, D. Olive, S. Perez, N. Pasqual, C. Faure, I. Ray-Coquard, A. Puisieux, C. Caux, J. Y. Blay, and C. Ménétrier-Caux. 2009. Regulatory T cells recruited through CCL22/CCR4 are selectively activated in lymphoid infiltrates surrounding primary breast tumors and lead to an adverse clinical outcome. *Cancer Res* 69: 2000-2009.

21. Lecoq, I., K. L. Kopp, M. Chapellier, P. Mantas, E. Martinenaite, M. Perez-Penco, L. Ronn Olsen, M. B. Zocca, A. Wakatsuki Pedersen, and M. H. Andersen. 2022. CCL22-based peptide vaccines induce anti-cancer immunity by modulating tumor microenvironment. *Oncoimmunology* 11: 2115655.

22. Li, Y. Q., F. F. Liu, X. M. Zhang, X. J. Guo, M. J. Ren, and L. Fu. 2013. Tumor secretion of CCL22 activates intratumoral Treg infiltration and is independent prognostic predictor of breast cancer. *PLoS One* 8: e76379.

23. Wang, Q., E. Schmoeckel, B. P. Kost, C. Kuhn, A. Vattai, T. Vilsmaier, S. Mahner, D. Mayr, U. Jeschke, and H. H. Heidegger. 2019. Higher CCL22+ Cell Infiltration is Associated with Poor Prognosis in Cervical Cancer Patients. *Cancers (Basel)* 11.

24. Wiedemann, G. M., M. M. Knott, V. K. Vetter, M. Rapp, S. Haubner, J. Fesseler, B. Kuhnemuth, P. Layritz, R. Thaler, S. Kruger, S. Ormanns, D. Mayr, S. Endres, and D. Anz. 2016. Cancer cell-derived IL-1alpha induces CCL22 and the recruitment of regulatory T cells. *Oncoimmunology* 5: e1175794.

25. Anz, D., M. Rapp, S. Eiber, V. H. Koelzer, R. Thaler, S. Haubner, M. Knott, S. Nagel, M. Golic, G. M. Wiedemann, F. Bauernfeind, C. Wurzenberger, V. Hornung, C. Scholz, D. Mayr, S. Rothenfusser, S. Endres, and C. Bourquin. 2015. Suppression of intratumoral

474 CCL22 by type i interferon inhibits migration of regulatory T cells and blocks cancer
475 progression. *Cancer Res* 75: 4483-4493.

476 26. Sugiyama, D., H. Nishikawa, Y. Maeda, M. Nishioka, A. Tanemura, I. Katayama, S.
477 Ezoe, Y. Kanakura, E. Sato, Y. Fukumori, J. Karbach, E. Jager, and S. Sakaguchi. 2013.
478 Anti-CCR4 mAb selectively depletes effector-type FoxP3+CD4+ regulatory T cells,
479 evoking antitumor immune responses in humans. *Proc Natl Acad Sci U S A* 110: 17945-
480 17950.

481 27. Wang, Q., K. Sudan, E. Schmoeckel, B. P. Kost, C. Kuhn, A. Vattai, T. Vilsmaier, S.
482 Mahner, U. Jeschke, and H. H. Heidegger. 2022. CCL22-Polarized TAMs to M2a
483 Macrophages in Cervical Cancer In Vitro Model. *Cells* 11.

484 28. Mantovani, A., P. A. Gray, J. Van Damme, and S. Sozzani. 2000. Macrophage-derived
485 chemokine (MDC). *J Leukoc Biol* 68: 400-404.

486 29. Yamashita, U., and E. Kuroda. 2002. Regulation of macrophage-derived chemokine
487 (MDC, CCL22) production. *Crit Rev Immunol* 22: 105-114.

488 30. Jung, M., and B. Bonavida. 2024. Immune Evasion in Cancer Is Regulated by Tumor-
489 Asociated Macrophages (TAMs): Targeting TAMs. *Crit Rev Oncog* 29: 1-17.

490 31. Liu, S., X. Cai, J. Wu, Q. Cong, X. Chen, T. Li, F. Du, J. Ren, Y. T. Wu, N. V. Grishin,
491 and Z. J. Chen. 2015. Phosphorylation of innate immune adaptor proteins MAVS,
492 STING, and TRIF induces IRF3 activation. *Science* 347: aaa2630.

493 32. Zhang, C., G. Shang, X. Gui, X. Zhang, X. C. Bai, and Z. J. Chen. 2019. Structural basis
494 of STING binding with and phosphorylation by TBK1. *Nature* 567: 394-398.

495 33. Lavoie, T. B., E. Kalie, S. Crisafulli-Cabatu, R. Abramovich, G. DiGioia, K. Moolchan,
496 S. Pestka, and G. Schreiber. 2011. Binding and activity of all human alpha interferon
497 subtypes. *Cytokine* 56: 282-289.

498 34. Schreiber, G. 2017. The molecular basis for differential type I interferon signaling. *The*
499 *Journal of Biological Chemistry* 292: 7285-7294.

500 35. Andersen, A. H. F., R. Olesen, K. L. Jonsson, J. F. Hojen, C. Krapp, K. Mack, M. K.
501 Thomsen, L. Ostergaard, M. Tolstrup, F. Dagnaes-Hansen, M. R. Jakobsen, and P. W.
502 Denton. 2019. cAIMP administration in humanized mice induces a chimerization-level-
503 dependent STING response. *Immunology* 157: 163-172.

504 36. Skouboe, M. K., A. Knudsen, L. S. Reinert, C. Boularan, T. Lioux, E. Perouzel, M. K.
505 Thomsen, and S. R. Paludan. 2018. STING agonists enable antiviral cross-talk between
506 human cells and confer protection against genital herpes in mice. *PLoS Pathog* 14:
507 e1006976.

508 37. Guerini, D. 2022. STING Agonists/Antagonists: Their Potential as Therapeutics and
509 Future Developments. *Cells* 11.

510 38. Motedayen Aval, L., J. E. Pease, R. Sharma, and D. J. Pinato. 2020. Challenges and
511 Opportunities in the Clinical Development of STING Agonists for Cancer
512 Immunotherapy. *J Clin Med* 9.

513 39. Su, T., Y. Zhang, K. Valerie, X. Y. Wang, S. Lin, and G. Zhu. 2019. STING activation in
514 cancer immunotherapy. *Theranostics* 9: 7759-7771.

515 40. Amouzegar, A., M. Chelvanambi, J. N. Filderman, W. J. Storkus, and J. J. Luke. 2021.
516 STING Agonists as Cancer Therapeutics. *Cancers (Basel)* 13.

517 41. Le Naour, J., L. Zitvogel, L. Galluzzi, E. Vacchelli, and G. Kroemer. 2020. Trial watch:
518 STING agonists in cancer therapy. *Oncoimmunology* 9: 1777624.

519 42. Wang, Y., Y. Zhu, Y. Cao, Y. Li, Z. Zhang, J. S. Fleishman, S. Cheng, J. Chen, and M.
520 Ding. 2025. The activation of cGAS-STING pathway offers novel therapeutic
521 opportunities in cancers. *Front Immunol* 16: 1579832.

522 43. Hines, J. B., A. J. Kacew, and R. F. Sweis. 2023. The Development of STING Agonists
523 and Emerging Results as a Cancer Immunotherapy. *Curr Oncol Rep* 25: 189-199.

524 44. Zhang, Y., Y. Wang, P. Mu, X. Zhu, and Y. Dong. 2024. Bidirectional regulation of the
525 cGAS-STING pathway in the immunosuppressive tumor microenvironment and its
526 association with immunotherapy. *Front Immunol* 15: 1470468.

527 45. Lemos, H., E. Mohamed, L. Huang, R. Ou, G. Pacholczyk, A. S. Arbab, D. Munn, and A.
528 L. Mellor. 2016. STING Promotes the Growth of Tumors Characterized by Low
529 Antigenicity via IDO Activation. *Cancer Res* 76: 2076-2081.

530 46. Liang, H., L. Deng, Y. Hou, X. Meng, X. Huang, E. Rao, W. Zheng, H. Mauceri, M.
531 Mack, M. Xu, Y. X. Fu, and R. R. Weichselbaum. 2017. Host STING-dependent MDSC
532 mobilization drives extrinsic radiation resistance. *Nat Commun* 8: 1736.

533 47. Ahn, J., T. Xia, H. Konno, K. Konno, P. Ruiz, and G. N. Barber. 2014. Inflammation-
534 driven carcinogenesis is mediated through STING. *Nat Commun* 5: 5166.

535 48. Ma, R., T. Ji, D. Chen, W. Dong, H. Zhang, X. Yin, J. Ma, X. Liang, Y. Zhang, G. Shen,
536 X. Qin, and B. Huang. 2016. Tumor cell-derived microparticles polarize M2 tumor-
537 associated macrophages for tumor progression. *Oncoimmunology* 5: e1118599.

538 49. Nakajima, S., K. Mimura, A. Kaneta, K. Saito, M. Katagata, H. Okayama, M. Saito, Z.
539 Saze, Y. Watanabe, H. Hanayama, T. Tada, W. Sakamoto, T. Momma, H. Ohira, and K.
540 Kono. 2023. Radiation-Induced Remodeling of the Tumor Microenvironment Through
541 Tumor Cell-Intrinsic Expression of cGAS-STING in Esophageal Squamous Cell
542 Carcinoma. *Int J Radiat Oncol Biol Phys* 115: 957-971.

543 50. Ma, F., B. Li, S. Y. Liu, S. S. Iyer, Y. Yu, A. Wu, and G. Cheng. 2015. Positive feedback
544 regulation of type I IFN production by the IFN-inducible DNA sensor cGAS. *J Immunol*
545 194: 1545-1554.

546 51. Ma, F., B. Li, Y. Yu, S. S. Iyer, M. Sun, and G. Cheng. 2015. Positive feedback
547 regulation of type I interferon by the interferon-stimulated gene STING. *EMBO Rep* 16:
548 202-212.

549 52. Le, E., F. Moadab, X. Wang, R. Najjar, S. J. Van den Bogaerde, A. Bays, J. LaCava, and
550 T. Mustelin. 2025. Interferons and Cytokines Induce Transcriptional Activation of the
551 Long-Interspersed Element-1 in Myeloid Cells from Autoimmune Patients. *Eur J*
552 *Immunol* 55: e2451351.

553 53. Ardeljan, D., M. S. Taylor, D. T. Ting, and K. H. Burns. 2017. The Human Long
554 Interspersed Element-1 Retrotransposon: An Emerging Biomarker of Neoplasia. *Clin*
555 *Chem* 63: 816-822.

556 54. Faffe, D. S., T. Whitehead, P. E. Moore, S. Baraldo, L. Flynt, K. Bourgeois, R. A.
557 Panettieri, and S. A. Shore. 2003. IL-13 and IL-4 promote TARC release in human
558 airway smooth muscle cells: role of IL-4 receptor genotype. *Am J Physiol Lung Cell Mol*
559 *Physiol* 285: L907-914.

560 55. Fujii-Maeda, S., K. Kajiwara, K. Ikizawa, M. Shinazawa, B. Yu, T. Koga, M. Furue, and
561 Y. Yanagihara. 2004. Reciprocal regulation of thymus and activation-regulated
562 chemokine/macrophage-derived chemokine production by interleukin (IL)-4/IL-13 and
563 interferon-gamma in HaCaT keratinocytes is mediated by alternations in E-cadherin
564 distribution. *J Invest Dermatol* 122: 20-28.

565 56. Fukuda, K., Y. Fujitsu, K. Seki, N. Kumagai, and T. Nishida. 2003. Differential
566 expression of thymus- and activation-regulated chemokine (CCL17) and macrophage-
567 derived chemokine (CCL22) by human fibroblasts from cornea, skin, and lung. *J Allergy*
568 *Clin Immunol* 111: 520-526.

569 57. Horikawa, T., T. Nakayama, I. Hikita, H. Yamada, R. Fujisawa, T. Bito, S. Harada, A.
570 Fukunaga, D. Chantry, P. W. Gray, A. Morita, R. Suzuki, T. Tezuka, M. Ichihashi, and
571 O. Yoshie. 2002. IFN-gamma-inducible expression of thymus and activation-regulated
572 chemokine/CCL17 and macrophage-derived chemokine/CCL22 in epidermal
573 keratinocytes and their roles in atopic dermatitis. *Int Immunol* 14: 767-773.

574 58. Bonecchi, R., S. Sozzani, J. T. Stine, W. Luini, G. D'Amico, P. Allavena, D. Chantry, and
575 A. Mantovani. 1998. Divergent effects of interleukin-4 and interferon-gamma on
576 macrophage-derived chemokine production: an amplification circuit of polarized T helper
577 2 responses. *Blood* 92: 2668-2671.

578 59. Xiao, T., S. Kagami, H. Saeki, M. Sugaya, T. Kakinuma, H. Fujita, S. Yano, H. Mitsui,
579 H. Torii, M. Komine, A. Asahina, K. Nakamura, and K. Tamaki. 2003. Both IL-4 and IL-
580 13 inhibit the TNF-alpha and IFN-gamma enhanced MDC production in a human
581 keratinocyte cell line, HaCaT cells. *J Dermatol Sci* 31: 111-117.

582 60. Faget, J., C. Biota, T. Bachelot, M. Gobert, I. Treilleux, N. Goutagny, I. Durand, S. Léon-
583 Goddard, J. Y. Blay, C. Caux, and C. Ménétrier-Caux. 2011. Early detection of tumor
584 cells by innate immune cells leads to T(reg) recruitment through CCL22 production by
585 tumor cells. *Cancer Res* 71: 6143-6152.

586 61. Blest, H. T. W., and L. Chauveau. 2023. cGAMP the travelling messenger. *Front*
587 *Immunol* 14: 1150705.

588 62. Carozza, J. A., V. Bohnert, K. C. Nguyen, G. Skariah, K. E. Shaw, J. A. Brown, M.
589 Rafat, R. von Eyben, E. E. Graves, J. S. Glenn, M. Smith, and L. Li. 2020. Extracellular
590 cGAMP is a cancer cell-produced immunotransmitter involved in radiation-induced anti-
591 cancer immunity. *Nat Cancer* 1: 184-196.

592 63. Mekers, V. E., V. M. Kho, M. Ansems, and G. J. Adema. 2022. cGAS/cGAMP/STING
593 signal propagation in the tumor microenvironment: Key role for myeloid cells in
594 antitumor immunity. *Radiother Oncol* 174: 158-167.

595 64. Ritchie, C., J. A. Carozza, and L. Li. 2022. Biochemistry, Cell Biology, and
596 Pathophysiology of the Innate Immune cGAS-cGAMP-STING Pathway. *Annu Rev*
597 *Biochem* 91: 599-628.

598 65. Wang, M., P. Xu, and Q. Wu. 2024. Cell-to-cell communications of cGAS-STING
599 pathway in tumor immune microenvironment. *Zhejiang Da Xue Xue Bao Yi Xue Ban* 53:
600 15-24.

601

602 **FIGURE LEGENDS**

603

604 **Figure 1. STING-activated macrophages and monocytes do not upregulate *CCL22*. *A)***
605 Microscopic images (20x brightfield) of THP-1 monocytes (upper left) and fully differentiated
606 THP-1-derived macrophages (lower right) are shown. ***B)*** THP-1-derived macrophages were
607 treated with cGAM(PS)2 (30 μM) for 24 hours, then harvested in TRIzol for RNA purification
608 and RTqPCR. Relative *CCL22* gene expression is shown. ***C)*** THP-1-derived macrophages were
609 treated with cGAM(PS)2 (30 μM) for 6 and 24 hours, then whole cell lysates (20 μg) and
610 antibody positive control (7 μg) were resolved with SDS-PAGE, transferred to nitrocellulose,
611 and probed for phosphorylated STING and beta-tubulin. ***D)*** THP-1 monocytes were treated with
612 cGAM(PS)2 (30 μM) and harvested for RTqPCR and *CCL22* gene expression as described in *B*.
613 Error bars represent standard deviations of independent biological replicates. Statistical analyses
614 were performed with unpaired, two-tailed *t* test (*B)* or non-parametric Wilcoxon signed-rank test
615 (*D*) due to non-Gaussian distribution of the treated sample per Shapiro-Wilk test.

616

617 **Figure 2. STING-activated macrophages and monocytes release factor(s) that upregulate**
618 ***CCL22* in cancer cells.** ***A)*** MCF7 and ***B)*** HeLa cells were treated for 24 hours with cGAM(PS)2
619 (30 μM) or conditioned media (CM) from macrophages that were either untreated or treated with
620 cGAM(PS)2 (30 μM) for 24 hours prior to media collection. Cells were harvested with TRIzol
621 for RNA purification and RTqPCR to assess relative expression of *CCL22.* ***C)*** MCF7 and ***D)***
622 HeLa cells were treated for 24 hours with cGAM(PS)2 (30 μM) or conditioned media (CM) from
623 monocytes that were either untreated or treated with cGAM(PS)2 (30 μM) for 24 hours prior to
624 media collection. Cells were harvested with TRIzol for RNA purification and RTqPCR to

625 determine expression of *CCL22* as above. For all figures, error bars represent standard deviations
626 of independent biological replicates. Statistical analyses were performed with one-way ANOVAs
627 on log-transformed data and Tukey's pairwise comparisons (*A*, *C*, and *D*) or with Brown-
628 Forsythe and Welch ANOVA (*B*) due to significant differences among standard deviations.
629
630 **Figure 3. Paracrine activation of *CCL22* in cancer cells activates STING and is dependent**
631 **on STING.** ***A)*** HeLa cells were treated for 24 hours with cGAM(PS)2 (30 μM) or conditioned
632 media (CM) from macrophages that were either untreated or treated with cGAM(PS)2 (30 μM)
633 for 24 hours. Whole cell lysates (25 μg) and antibody positive control (5 μg) were resolved with
634 SDS-PAGE, transferred to nitrocellulose and probed for phosphorylated STING and beta-
635 tubulin. The image shown is representative of at least three independent experiments. ***B)*** HeLa$^{-/-}$
636 ^{TMEM173} STING knockout cells were treated for 24 hours with cGAM(PS)2 (30 μM) or
637 conditioned media (CM) from macrophages that were either untreated or treated with
638 cGAM(PS)2 (30 μM) for 24 hours prior to media collection. Cells were harvested with TRIzol
639 for RNA purification and RTqPCR to determine relative expression of *CCL22*. Error bars
640 represent standard deviations of independent biological replicates. Statistical analysis was
641 performed using one-way ANOVA and Tukey's pairwise comparisons.
642
643 **Figure 4. Type I IFNs have modest effects on *CCL22* in HeLa cells that remain STING-**
644 **dependent.** HeLa ***(A-B)*** and MCF7 cells ***(C- D)*** were treated with exogenous type I IFNs at
645 indicated concentrations for 48 (HeLa) or 24 hours (MCF7), then harvested with TRIzol for
646 RNA purification and RTqPCR to determine relative gene expression of *CCL22*. ***E-F)*** HeLa $^{-/-}$
647 ^{TMEM173} STING knockout cells were treated with exogenous type I IFNs at indicated

648 concentrations for 48 hours, then harvested with TRIzol for RNA purification and RTqPCR
649 analysis of *CCL22.* Error bars represent standard deviations of independent biological replicates.
650 Statistical analyses were performed using one-way ANOVA with Dunnett's multiple
651 comparisons test (*A, C, E*), one-way ANOVA on log-transformed data with Tukey's pairwise
652 comparisons (*B, D*), and unpaired, two-tailed t test (*F*). ***G)*** HeLa wild type cells were treated
653 with IFNβ (100 ng/mL) for 48 hours, and whole cell lysates (60 μg) and antibody positive
654 control (5 μg) were resolved with SDS-PAGE, transferred to nitrocellulose and probed for
655 phosphorylated STING and beta-tubulin. ***H)*** HeLa wild type (WT) and HeLa $^{-/-TMEM173}$ STING
656 knockout (KO) cells were treated as indicated for approximately 30 hours prior to harvesting;
657 whole cell lysates (15 μg) were resolved with SDS-PAGE, transferred to nitrocellulose, and
658 probed for phosphorylated Stat1 and beta-tubulin. ***I)*** HeLa cells were pretreated for 3 hours with
659 MMHAR-2 neutralizing antibody, then indicated treatments were added, including conditioned
660 media (CM) from macrophages treated with cGAM(PS)2 (30 μM), and cells were incubated for
661 approximately 48 hours prior to harvest in TRIzol for RNA purification and RTqPCR to assess
662 relative changes in *CCL22* expression. Statistical analyses were performed using one-way
663 ANOVA with Šídák's multiple comparisons test.
664
665 **Figure 5. STING agonists differentially upregulate *CCL22* and *IFNβ*.** HeLa ***(A-D)*** and
666 MCF7 cells ***(E-H)*** were treated with 30 μM of each indicated STING agonist or DMSO vehicle
667 control (for diABZI) for 24 hours, then harvested in TRIzol for RNA purification and RTqPCR
668 using TaqMan assays for *CCL22* or *IFNb*. Error bars represent standard deviations of
669 independent biological replicates. Statistical analyses were performed on log-transformed data

670 using unpaired, two-tailed t tests except for *C* and *G*, which were analyzed with a one-way

671 ANOVA and Šídák's multiple comparisons test.

Fig. 1

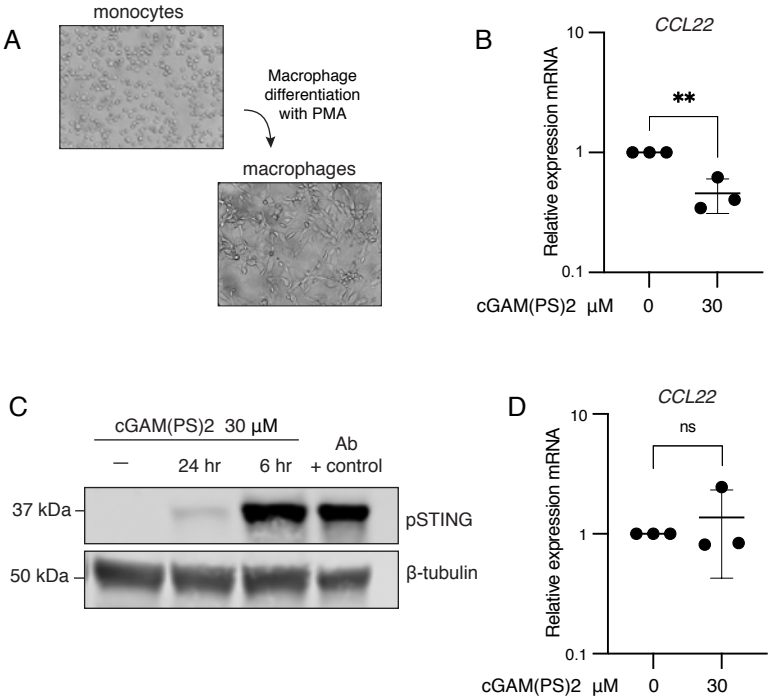
A
monocytes
Macrophage differentiation with PMA
macrophages
B
CCL22
Relative expression mRNA
10
1
0.1
**
cGAM(PS)2 μM
0
30
C
cGAM(PS)2 30 μM
—
24 hr
6 hr
Ab + control
37 kDa
pSTING
50 kDa
β-tubulin
D
CCL22
Relative expression mRNA
10
1
0.1
ns
cGAM(PS)2 μM
0
30

Fig. 2

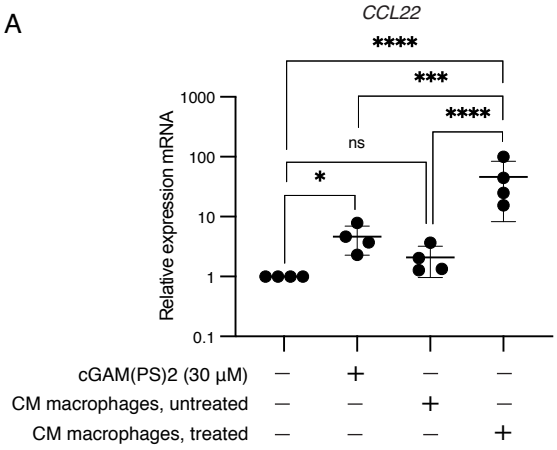
A
CCL22
****
***
****
ns
*
Relative expression mRNA
1000
100
10
1
0.1
cGAM(PS)2 (30 μM) – + – –
CM macrophages, untreated – – + –
CM macrophages, treated – – – +

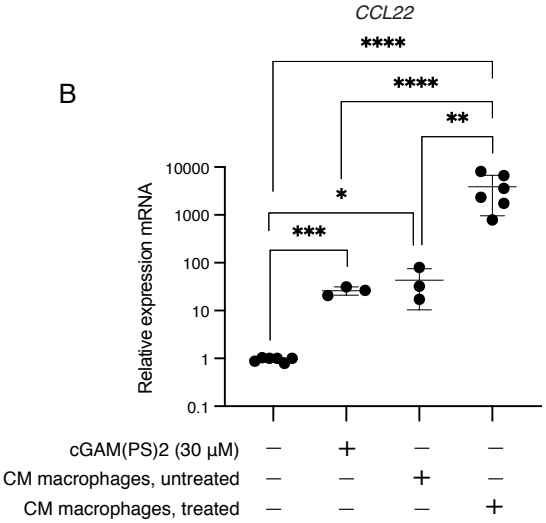
B
CCL22
****
****
**
*
***
Relative expression mRNA
10000
1000
100
10
1
0.1
cGAM(PS)2 (30 μM) – + – –
CM macrophages, untreated – – + –
CM macrophages, treated – – – +

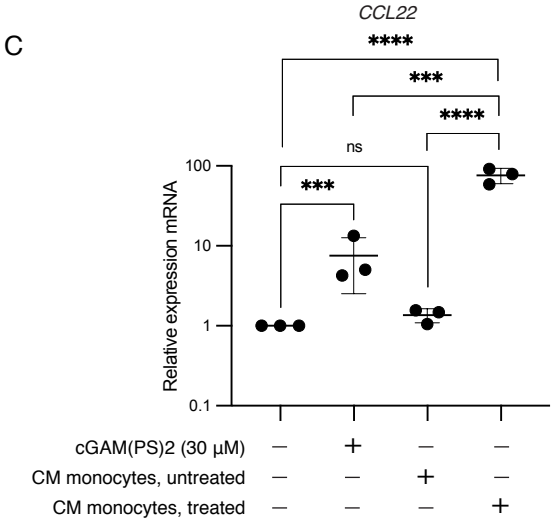
C
CCL22
****
***
****
ns
***
Relative expression mRNA
100
10
1
0.1
cGAM(PS)2 (30 μM) – + – –
CM monocytes, untreated – – + –
CM monocytes, treated – – – +

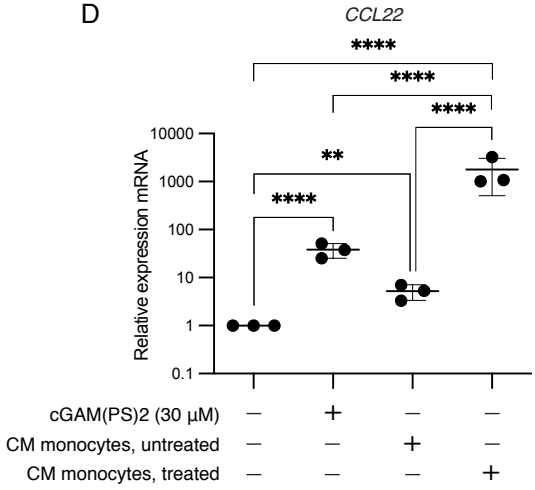
D
CCL22
****
****
****
**
****
Relative expression mRNA
10000
1000
100
10
1
0.1
cGAM(PS)2 (30 μM) – + – –
CM monocytes, untreated – – + –
CM monocytes, treated – – – +

Fig. 3

A

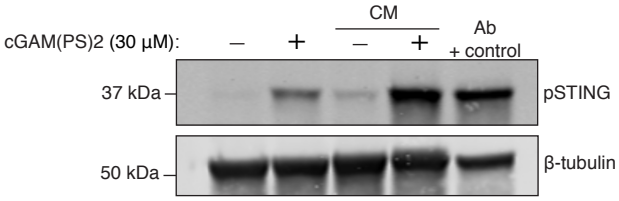
CM
cGAM(PS)2 (30 μM):
–
+
–
+
Ab
+ control
37 kDa
pSTING
50 kDa
β-tubulin

B

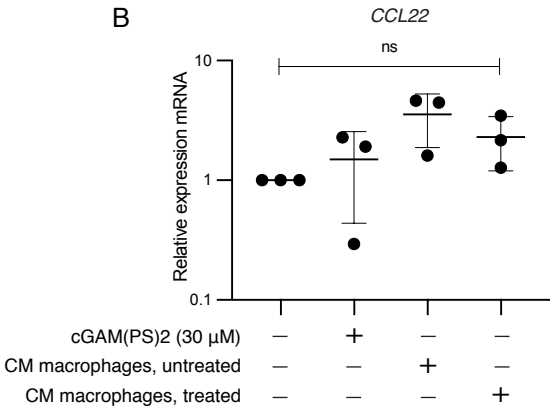
CCL22
ns
Relative expression mRNA
10
1
0.1
cGAM(PS)2 (30 μM)
CM macrophages, untreated
CM macrophages, treated

Fig. 4

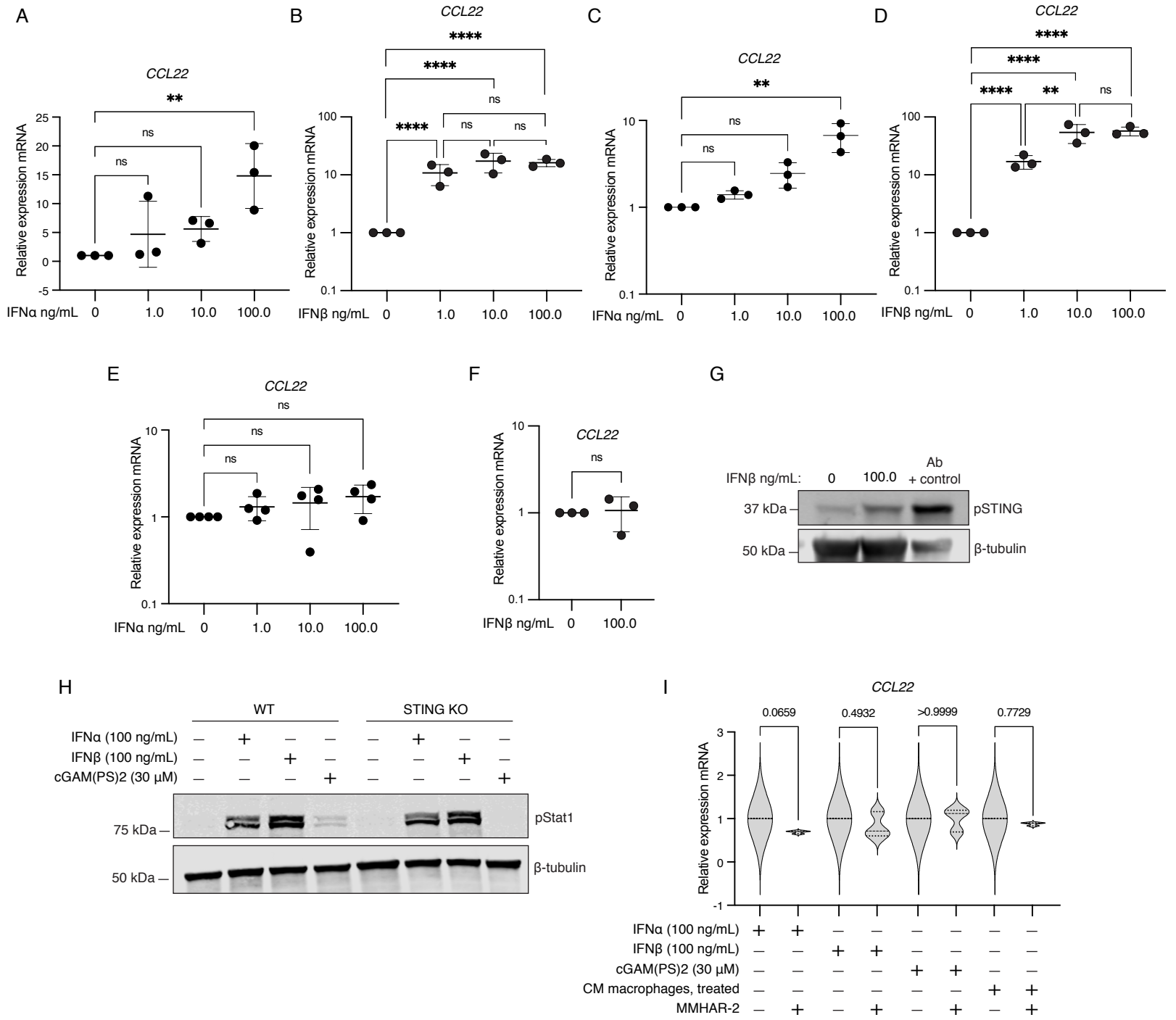
A
CCL22
Relative expression mRNA
IFNα ng/mL 0 1.0 10.0 100.0
B
CCL22
IFNβ ng/mL 0 1.0 10.0 100.0
C
CCL22
IFNα ng/mL 0 1.0 10.0 100.0
D
CCL22
IFNβ ng/mL 0 1.0 10.0 100.0
E
CCL22
IFNα ng/mL 0 1.0 10.0 100.0
F
CCL22
IFNβ ng/mL 0 100.0
G
IFNβ ng/mL: 0 100.0 Ab + control
37 kDa
pSTING
50 kDa
β-tubulin
H
WT
STING KO
IFNα (100 ng/mL)
IFNβ (100 ng/mL)
cGAM(PS)2 (30 μM)
75 kDa
pStat1
50 kDa
β-tubulin
I
CCL22
0.0659
0.4932
>0.9999
0.7729
Relative expression mRNA
IFNα (100 ng/mL)
IFNβ (100 ng/mL)
cGAM(PS)2 (30 μM)
CM macrophages, treated
MMHAR-2

Fig. 5

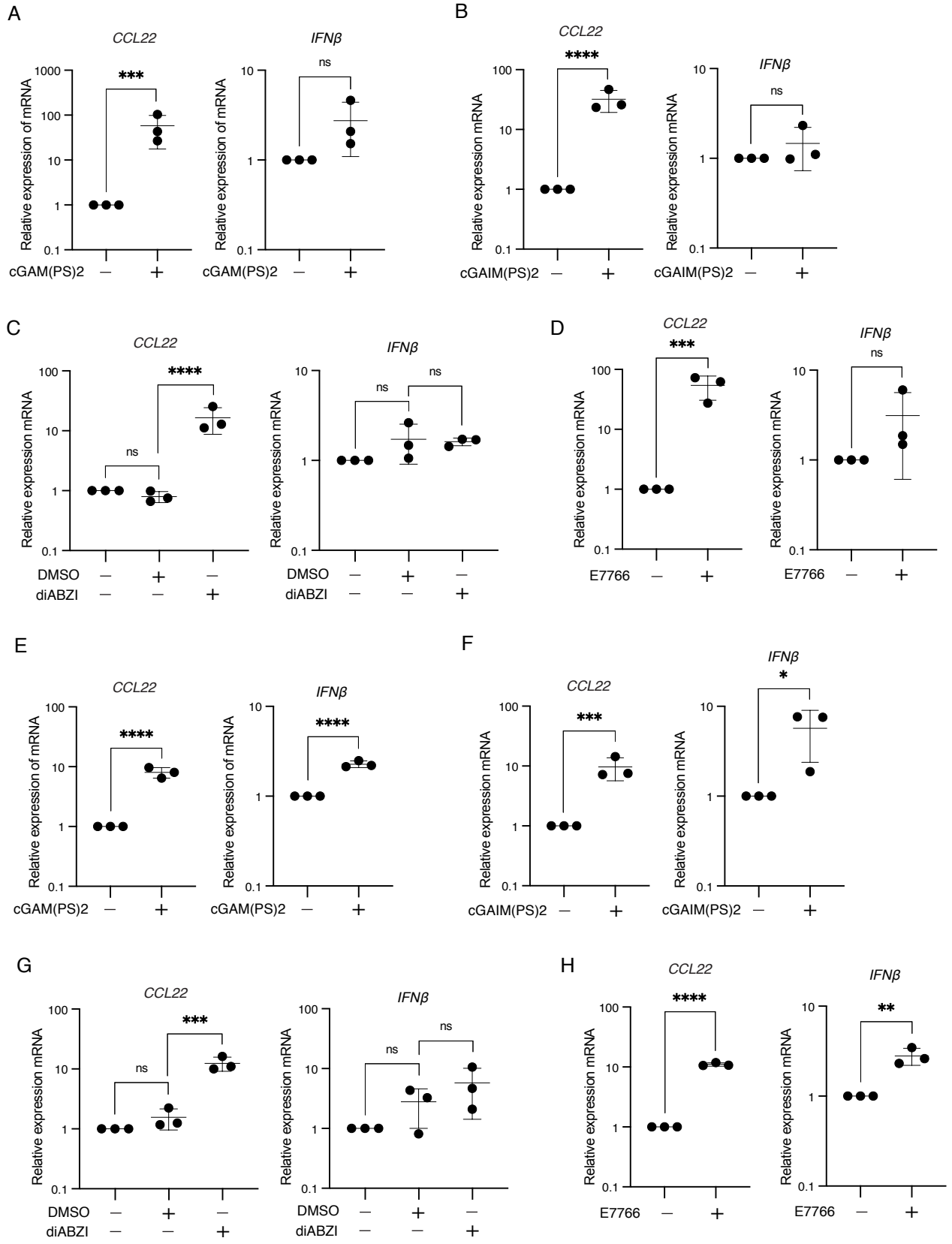
A
CCL22
IFNβ
Relative expression of mRNA
***
ns
cGAM(PS)2 – +
B
CCL22
IFNβ
Relative expression mRNA
****
ns
cGAIM(PS)2 – +
C
CCL22
IFNβ
Relative expression mRNA
****
ns
DMSO – + –
diABZI – – +
D
CCL22
IFNβ
Relative expression mRNA
***
ns
E7766 – +
E
CCL22
IFNβ
Relative expression of mRNA
****
cGAM(PS)2 – +
F
CCL22
IFNβ
Relative expression mRNA
***
*
cGAIM(PS)2 – +
G
CCL22
IFNβ
Relative expression mRNA
***
ns
DMSO – + –
diABZI – – +
H
CCL22
IFNβ
Relative expression mRNA
****
**
E7766 – +

Fig. S1

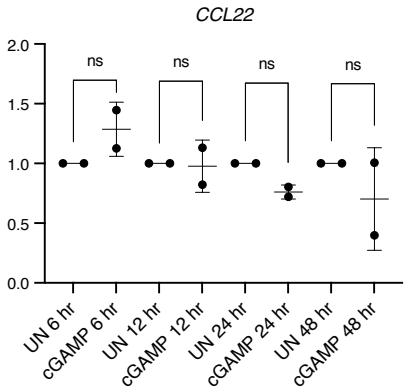

Supplementary Figure 1. THP-1-derived macrophages were untreated (UN) or treated with cGAM(PS)2 (30 μM) for indicated times, then harvested in TRIzol for RNA purification and RTqPCR. Relative gene expression of *CCL22* is shown. Error bars represent standard deviations of independent biological replicates. Statistical significnace was determined uisng Kruskal-Wallis multiple comparisons test.

Fig. S2

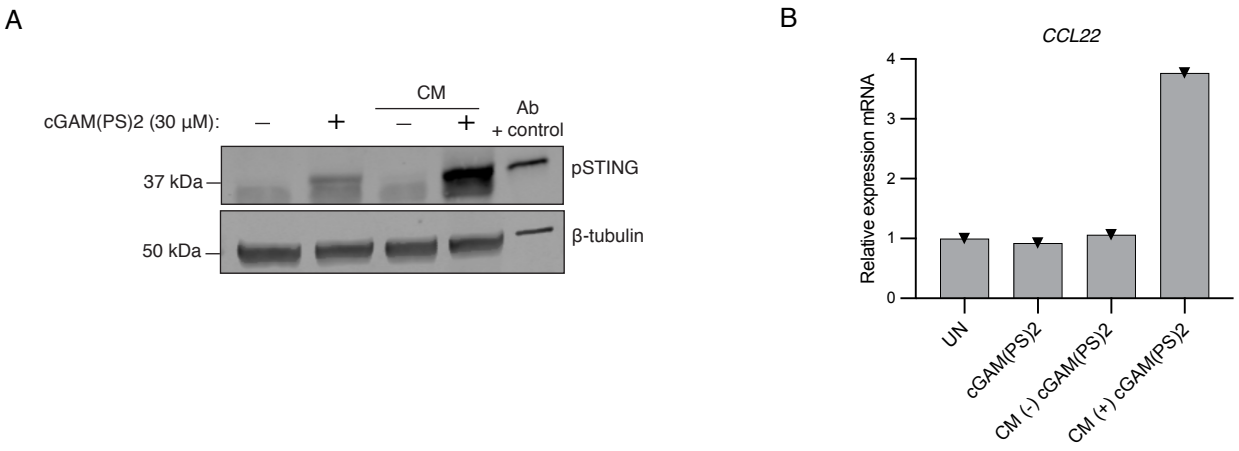

Supplementary Figure 2. ***A)*** HeLa cells (wild type) were untreated or treated for 24 hours with either cGAM(PS)2 (30 μM) or conditioned media (CM) from untreated monocytes or monocytes treated with cGAM(PS)2 (30 μM) for 24 hours. Whole cell lysates (60 μg) and antibody positive control (15 μg) were resolved with SDS-PAGE, transferred to nitrocellulose and probed for phosphorylated STING and beta-tubulin. ***B)*** HeLa $^{-/-\ TMEM173}$ (STING KO) cells were untreated or treated with either cGAM(PS)2 (30 μM) or conditioned media (CM) from untreated monocytes or monocytes treated with cGAM(PS)2 (30 μM) for 24 hours. Cells were harvested in TRIzol for RNA purification and RTqPCR to determine relative levels of *CCL22*.

Fig. S3

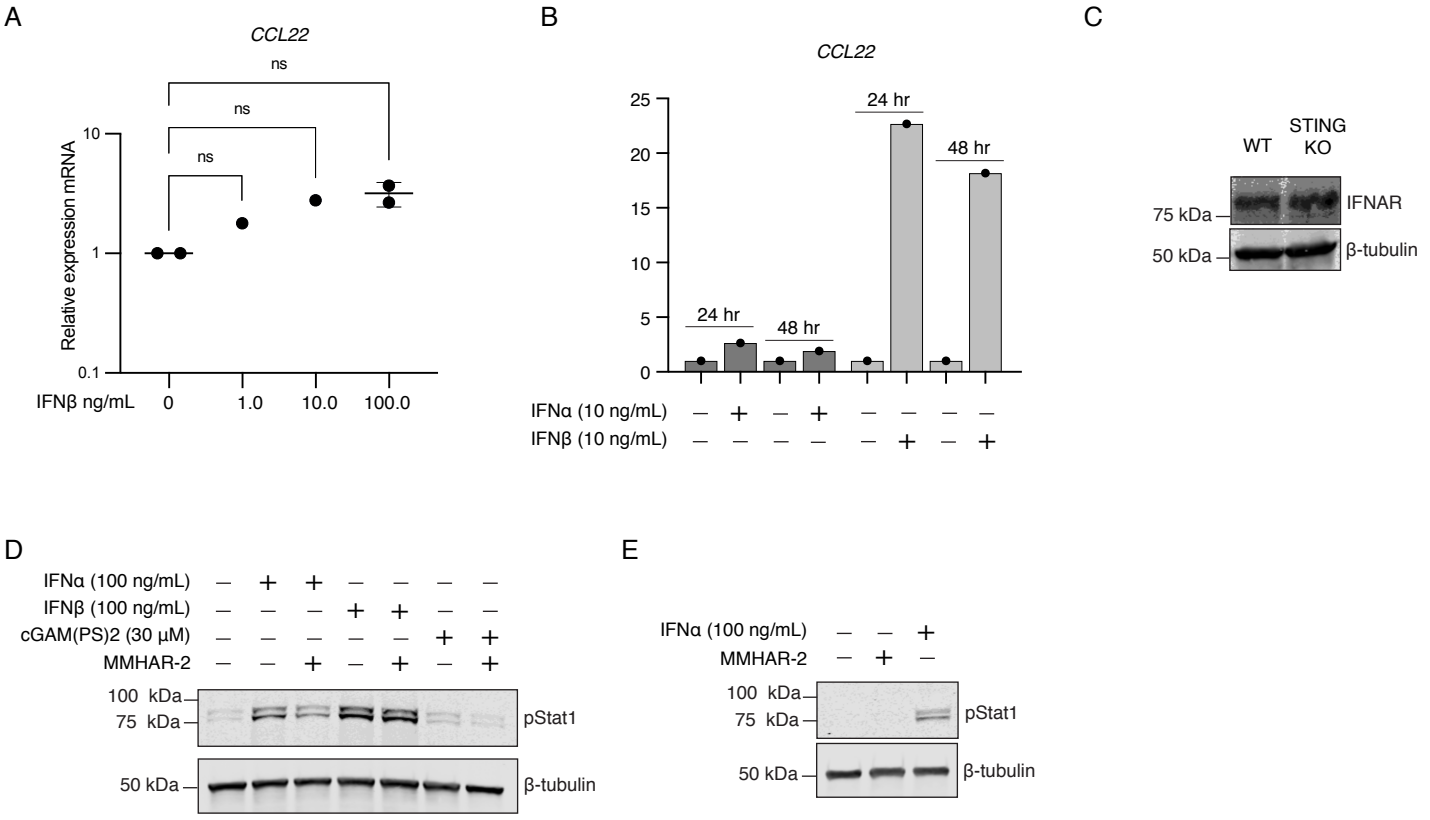

Supplementary Figure 3. ***A)*** HeLa cells were treated for 24 hours with exogenous IFNβ at indicated concentrations, then harvested in TRIzol for RNA purification and RTqPCR to assess relative fold changes in *CCL22* expression. Error bars represent standard deviations of independent biological replicates, and statistical analysis was performed with one-way ANOVA and Dunnett's pairwise comparsions. ***B)*** MCF7 cells were treated for 24 or 48 hours with 10 ng/mL of IFNα or IFNβ, then harvested for RTqPCR as in *A*. ***C)*** Whole cell lysates (40 μg) from HeLa wild type (WT) and HeLa $^{-/-TMEM173}$ STING knock out (KO) cells were resolved with SDS-PAGE, transferred to nitrocellulose, and probed for IFNAR2 and beta-tubulin. ***D-E)*** HeLa cells were pretreated for 3 hours with MMHAR-2 neutralizing antibody, then indicated treatments were added and cells incubated for approximately 48 hours, at which time whole cell lysates (5 μg) were resolved with SDS-PAGE, transfered to nitrocellulose and probed with anti-pStat1 and β-tubulin.